

See discussions, stats, and author profiles for this publication at: <https://www.researchgate.net/publication/6892480>

Monolayered Organosilicate Toroids and Related Structures: A Phase Diagram for Templating from Block Copolymers

ARTICLE *in* NANO LETTERS · SEPTEMBER 2006

Impact Factor: 13.59 · DOI: 10.1021/nl0612906 · Source: PubMed

CITATIONS

19

READS

18

8 AUTHORS, INCLUDING:



Thomas M Hermans

University of Strasbourg

19 PUBLICATIONS 392 CITATIONS

SEE PROFILE



Geraud Dubois

IBM

69 PUBLICATIONS 1,264 CITATIONS

SEE PROFILE



Jane Frommer

IBM

88 PUBLICATIONS 3,893 CITATIONS

SEE PROFILE



Robert M Waymouth

Stanford University

277 PUBLICATIONS 15,545 CITATIONS

SEE PROFILE

Monolayered Organosilicate Toroids and Related Structures: A Phase Diagram for Templating from Block Copolymers

Jeongsoo Choi,[†] Thomas M. Hermans,[†] Bas G. G. Lohmeijer,[†] Russell C. Pratt,[†] Geraud Dubois,[†] Jane Frommer,[†] Robert M. Waymouth,[‡] and James L. Hedrick^{*,†}

IBM Almaden Research Center, 650 Harry Road, San Jose, California 95120, and
Department of Chemistry, Stanford University, Stanford, California 94305

Received June 5, 2006; Revised Manuscript Received July 10, 2006

ABSTRACT

Here we report the controlled generation of micelle-templated organosilicate nanostructures resulting from self-assembly of a block copolymer/organosilicate mixture followed by organosilicate vitrification and copolymer thermolysis. Variation of solution condition and the copolymer/organosilicate mixture composition generates widely different film morphologies ranging from toroids to linear features to contiguous nanoporous monolayers. The use of reactive organosilicates for block copolymer templation generates functional inorganic nanostructures with thermal and mechanical stability.

The formation of nanostructured materials via self-assembly using amphiphilic molecules has attracted significant attention owing to the wide range of applications from etch masks for nanolithography to templates for nanomaterial synthesis and pharmaceutical formulations.^{1–4} Compared to conventional amphiphiles such as low molecular weight surfactants and lipids, block copolymers offer advantages in tuning their shape and functionality as their chemical structure, composition, size, and architecture are varied systematically.^{5–7} Recent studies have enriched the scope of block copolymer self-assembly by increasing the diversity of supramolecular aggregates such as micelles,^{8–10} vesicles,^{7,10–14} and toroids^{15–19} formed in both aqueous and organic environments. In selective solvents, block copolymers can manifest various micellar morphologies including spheres, cylinders, or vesicles, depending on both intrinsic properties such as the block–block interaction parameter, χ , and extrinsic properties such as overall molecular weight, block composition, solvent composition, and concentration. For example, LaRue et al. reported that the micellar structure of poly(styrene-*block*-isoprene) in heptane changed from spheres to wormlike cylinders by either reducing the isoprene corona length²⁰ or changing temperature.²¹ Manners et al. reported a range of morphologies of organosilane-based amphiphilic block copolymers in water and dioxane/water mixed solvent.^{22–24} Eisenberg et al. showed a morphological transition of poly(styrene-*block*-acrylic acid) micelles in a water/*N,N*-dimeth-

ylformamide (DMF) solvent mixture from spheres to cylinders to vesicles as the water fraction in the mixture increased.^{25,26} Lodge et al. reported a three-dimensional phase diagram of the block copolymer morphology for a poly(styrene-*block*-isoprene) copolymer that depended on both the solvent composition and polymer concentration.^{27,28} The formation of multicompartment micelles from ABC triblock terpolymers comprising a hydrocarbon, a fluorocarbon, and a water-soluble block has been reported by Hillmyer and Lodge.^{8–10} The utility of selectively cross-linking the individual components of such self-assembled nanostructures has been shown by Wooley,^{29–31} where stability, subsequent functionalization, and application in diverse environments have been demonstrated. In particular, Wooley and Pochan demonstrated that poly(acrylic acid-*block*-methyl methacrylate-*block*-styrene) is capable of forming toroids (donuts) whose morphology could be preserved by cross-linking.^{15,16} In addition, there have been several reports on the deposition of block copolymer micelles on surfaces to obtain nanostructures for making nanoparticle arrays³² and other functional or responsive surfaces.³³ However, a simple method to prepare micelle-templated inorganic nanostructures has not appeared. Here, we report the controlled generation of micelle-templated organosilicate nanostructures from binary mixtures of a block copolymer and an organosilicate precursor. This strategy is based on the self-assembly of a hydrophilic/hydrophobic block copolymer where the organosilicate is selectively sequestered into the polar block of the copolymer. We also demonstrate a simple method to generate widely different morphologies ranging from toroids

* Corresponding author. Tel: 408-927-1632. Fax: 408-927-3310.
E-mail: hedrick@almaden.ibm.com.

[†] IBM Almaden Research Center.

[‡] Stanford University.

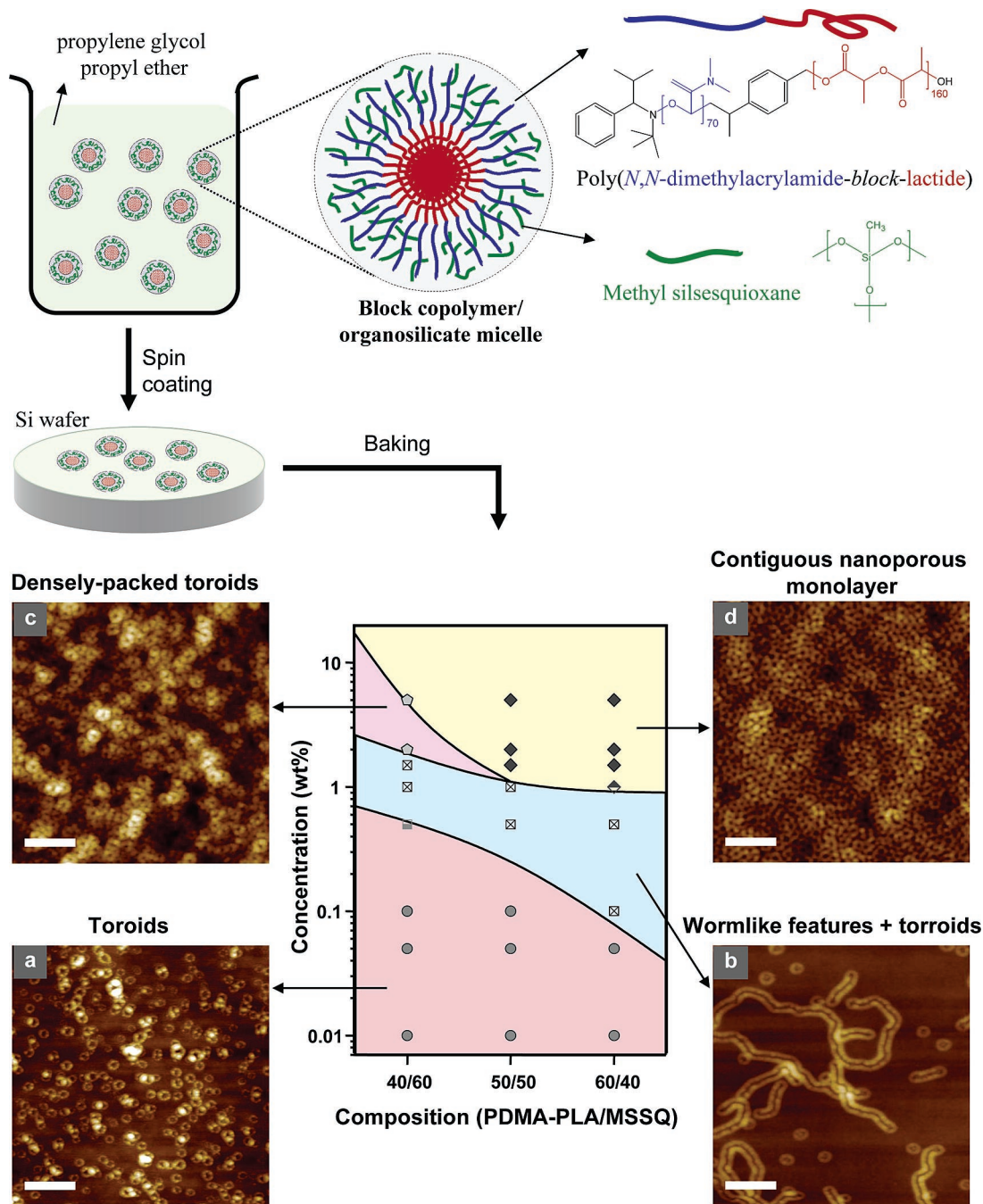


Figure 1. Schematic illustration of the general procedure to produce nanostructured thin films (upper part) and their resulting morphologies (lower part). The nanostructures are formed by a spinning PEPE solution of PDMA-PLA and MSSQ onto a silicon wafer under varied conditions of solution concentration and mixture composition. Panels a–d are AFM images corresponding to each region of the morphological diagram, XY scale bar = 300 nm, $z = 10$ nm (a, c, d) and 40 nm (b).

to linear wormlike features to densely packed toroids to contiguous nanoporous monolayers.

An amphiphilic poly(*N,N*-dimethylacrylamide-*block-rac*-lactide) copolymer (PDMA₇₀-PLA₁₅₀) having a molecular weight of 47100 g mol⁻¹ and a polydispersity index of 1.11 is used in this study (see Supplementary Information for experimental details).³⁴ We have reported the self-assembly of PDMA-PLA block copolymer/methyl silsesquioxane (MSSQ) mixtures in propylene glycol propyl ether (PGPE) to generate micelles with a PLA core and a PDMA/MSSQ corona and their use to generate highly porous low dielectric

constant materials for microelectronic applications.³⁴ While the PDMA-PLA/MSSQ mixtures generated spherical micelles that could be transferred onto a silicon wafer as a relatively thick film (250–400 nm) by using higher concentration solutions (10 wt %),³⁴ herein we report the markedly different behavior observed when this formulation is prepared as ultrathin films (<25 nm) from very low solution concentrations. The composite is formulated at 40:60, 50:50, or 60:40 copolymer/MSSQ by weight, and the concentration of the composite in PGPE solutions was varied from 0.001 to 5 wt %. Thin films are prepared by spin

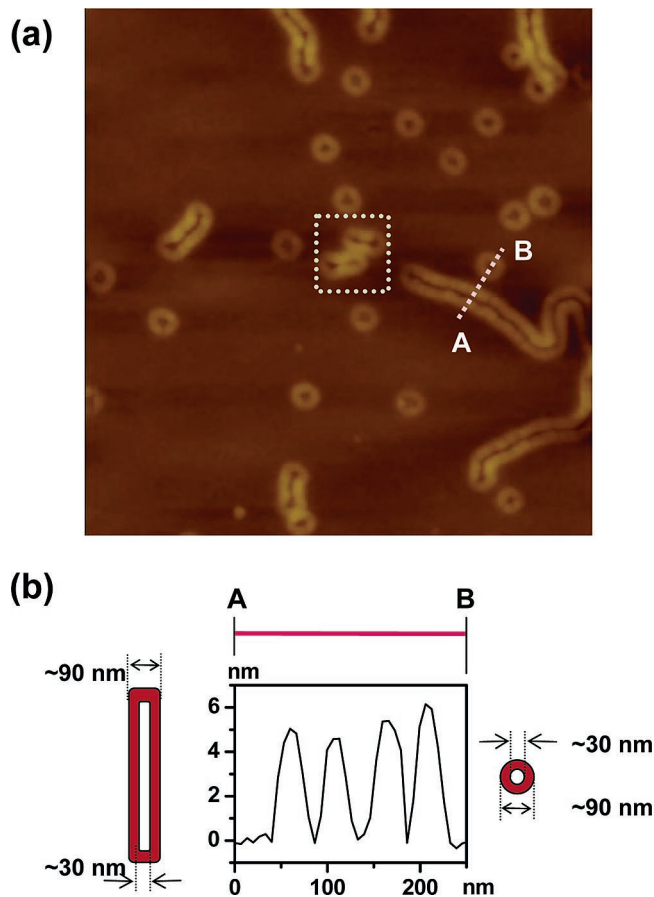


Figure 2. (a) AFM image of surface prepared from 0.5 wt % PGPE solution of PDMA-PLA/MSSQ=50/50 (XY scale = $1.5\ \mu\text{m} \times 1.5\ \mu\text{m}$ and Z scale = 40 nm). (b) Height profiles taken from the line A–B with corresponding schematic illustrations of toroid and wormlike linear feature, respectively.

coating these PGPE solutions onto untreated silicon wafers at 3000 rpm. The spin-coated wafers are heated to 450 °C at 10 °C/min under nitrogen to initiate vitrification of the MSSQ and formation of the inorganic network and then held at 450 °C for 2 h under nitrogen to degrade the copolymer template and produce organosilicate thin films. Figure 1 illustrates the micelle-directed assembly of organosilicate precursors, vitrification of organosilicates, followed by micelle thermolysis to generate the inorganic nanostructures.

Characterization of the surface by atomic force microscopy (AFM) shows the presence of four distinct morphologies: isolated toroids, linear wormlike features, densely packed toroids, and contiguous nanoporous films. At very low concentrations (≤ 0.1 wt %), isolated toroids predominate for all compositions. The size of the toroids is regular and reproducible, with the outer diameters averaging 70 nm and inner diameters averaging 30 nm as depicted in Figure 1a. At intermediate concentrations ($\sim 0.1 < C < \sim 1.5$ wt %) toroids are mixed with wormlike linear features that have a continuous open channel down their length as shown in Figure 1b. It is noteworthy that the dimensions of the coexisting toroids and linear features are similar: the outer widths are 90 nm and the widths of their internal channels/voids are 30 nm (Figure 2). This similarity suggests that the linear features form by fusion of toroids with a proposed

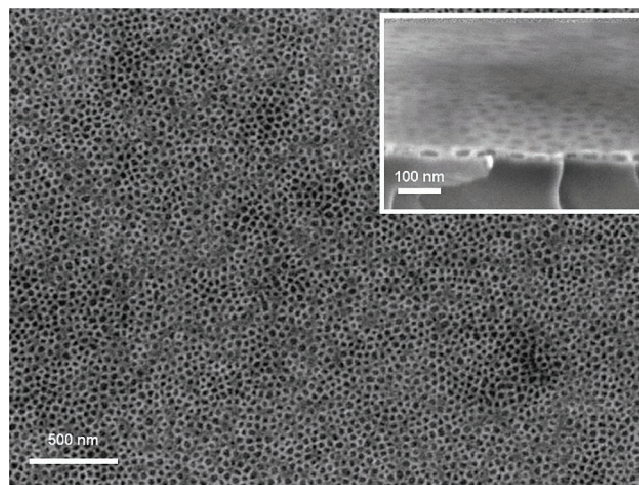


Figure 3. Top-view and plane-view (inset) SEM micrographs of contiguous nanoporous film prepared from 2.0 wt % PGPE solution of PDMA-PLA/MSSQ = 60/40 mixture.

intermediate stage presented inside the dotted box in Figure 2a and in Figure S2.

At higher concentrations ($C > 1.5$ wt %), the fraction of MSSQ in the mixture affects the resulting morphology of toroid packing rather significantly (parts c and d of Figure 1). With higher fractions of MSSQ in the mixture, toroids densely pack while maintaining their original shape as toroids. With lower fractions of MSSQ in the mixture, a contiguous film with a uniform distribution of pores is obtained. Figure 3 shows a top-view SEM image of this film with a narrow distribution of uniform size pores (~ 30 nm). In a cross-sectional view (Figure 3 inset), also illustrated is the confinement of the nanoporous film to a single layer on the substrate, a feature of benefit to future applications such as etch masks for nanolithography.

Thin film morphologies can be correlated to composition and concentration as shown in the rudimentary phase diagram of Figure 1. In our experiments, solution concentration is found to play a more decisive role than composition in determining morphologies of nanostructures, especially in a dilute concentration regime. The lower part of Figure 1 shows a diagram of micelle-templated nanostructures prepared by varying both composition and concentration with representative morphological features of each region as recorded by AFM (see also Figure 1S shown with all AFM images corresponding to a wider range of concentration). Although the stable and reproducible formation of toroidal microstructures on surfaces is well documented, the driving force for the transitions between the various morphological phases is not fully understood and is currently under investigation.

In summary, nanostructured organosilicate thin films can be formed via coassembly of an organosilicate precursor and PDMA-PLA copolymers in a selective solvent. Variations in the solution concentration and mixture composition give control over the nanostructure morphology formed on silicon wafer surfaces, allowing access to isolated toroids, linear wormlike features, densely packed toroids, or contiguous nanoporous monolayer films. For producing toroids in particular, this method offers the advantages of control over

uniformity in shape and size, and straightforward preparation. The use of the thermosetting organosilicate, selectively sequestered into the PDMA phase during coassembly, allows fossilization of the self-assembled structures into robust nanostructures with thermal and mechanical stability suitable for application as etching masks in microelectronics.

Acknowledgment. The authors acknowledge support from the NSF Center for Polymer Interfaces and Macromolecular Assemblies (CPIMA: NSF-DMR-0213618). This work was also partially supported by the Korea Research Foundation Grant funded by the Korean Government (MOEHRD) (KRF-2005-214-D00273).

Supporting Information Available: Description of experimental methods, a morphology phase diagram of nanostructures, and a magnified image from Figure 2a with height profiles. This material is available free of charge via the Internet at <http://pubs.acs.org>.

References

- (1) Park, M.; Harrison, C.; Chaikin, P. M.; Register, R. A.; Adamson, D. H. *Science* **1997**, *276*, 1401.
- (2) Alexandridis, P.; Lindman, B. *Amphiphilic Block Copolymers: Self-Assembly and Applications*; Elsevier Science: Amsterdam, 2000.
- (3) Huang, E.; Rockford, L.; Russell, T. P.; Hawker, C. J. *Nature* **1998**, *395*, 757.
- (4) Thurn-Albrecht, T.; Steiner, R.; DeRouchey, J.; Stafford, C. M.; Huang, E.; Bal, M.; Tuominen, M.; Hawker, C. J.; Russell, T. *Adv. Mater.* **2000**, *12*, 787.
- (5) Hawker, C. J.; Wooley, K. L. *Science* **2005**, *309*, 1200.
- (6) Segalman, R. A. *Mater. Sci. Eng., R* **2005**, *48*, 191.
- (7) Forster, S.; Antonietti, M. *Adv. Mater.* **1998**, *10*, 195.
- (8) Li, Z. B.; Kesselman, E.; Talmon, Y.; Hillmyer, M. A.; Lodge, T. P. *Science* **2004**, *306*, 98.
- (9) Lodge, T. P.; Rasdal, A.; Li, Z. B.; Hillmyer, M. A. *J. Am. Chem. Soc.* **2005**, *127*, 17608.
- (10) Li, Z. B.; Hillmyer, M. A.; Lodge, T. P. *Macromolecules* **2006**, *39*, 765.
- (11) Riess, G. *Prog. Polym. Sci.* **2003**, *28*, 1107.
- (12) Potemkin, I. I.; Moller, M. *Macromolecules* **2005**, *38*, 2999.
- (13) Kastle, G.; Boyen, H. G.; Weigl, F.; Lengel, G.; Herzog, T.; Ziemann, P.; Riethmuller, S.; Mayer, O.; Hartmann, C.; Spatz, J. P.; Moller, M.; Ozawa, M.; Banhart, F.; Garnier, M. G.; Oelhafen, P. *Adv. Funct. Mater.* **2003**, *13*, 853.
- (14) Gohy, J. F.; Willet, N.; Varshney, S.; Zhang, J. X.; Jerome, R. *Angew. Chem., Int. Ed.* **2001**, *40*, 3214.
- (15) Pochan, D. J.; Chen, Z. Y.; Cui, H. G.; Hales, K.; Qi, K.; Wooley, K. L. *Science* **2004**, *306*, 94.
- (16) Chen, Z. Y.; Cui, H. G.; Hales, K.; Li, Z. B.; Qi, K.; Pochan, D. J.; Wooley, K. L. *J. Am. Chem. Soc.* **2005**, *127*, 8592.
- (17) Forster, S.; Hermsdorf, N.; Leube, W.; Schnablegger, H.; Regensbrecht, M.; Akari, S.; Lindner, P.; Bottcher, C. *J. Phys. Chem. B* **1999**, *103*, 6657.
- (18) Netz, R. R. *Europhys. Lett.* **1999**, *47*, 391.
- (19) Jiang, Y.; Zhu, J. T.; Jiang, W.; Liang, H. J. *J. Phys. Chem. B* **2005**, *109*, 21549.
- (20) LaRue, I.; Adam, M.; da Silva, M.; Sheiko, S. S.; Rubinstein, M. *Macromolecules* **2004**, *37*, 5002.
- (21) LaRue, I.; Adam, M.; Pitsikalis, M.; Hadjichristidis, N.; Rubinstein, M.; Sheiko, S. S. *Macromolecules* **2006**, *39*, 309.
- (22) Arsenaault, A. C.; Rider, D. A.; Tetreault, N.; Chen, J. I. L.; Coombs, N.; Ozin, G. A.; Manners, I. *J. Am. Chem. Soc.* **2005**, *127*, 9954.
- (23) Wang, X. S.; Winnik, M. A.; Manners, I. *Macromolecules* **2005**, *38*, 1928.
- (24) Wang, X. S.; Winnik, M. A.; Manners, I. *Angew. Chem., Int. Ed.* **2004**, *43*, 3703.
- (25) Zhang, L. F.; Eisenberg, A. *J. Am. Chem. Soc.* **1996**, *118*, 3168.
- (26) Yu, K.; Eisenberg, A. *Macromolecules* **1998**, *31*, 3509.
- (27) Hanley, K. J.; Lodge, T. P.; Huang, C. I. *Macromolecules* **2000**, *33*, 5918.
- (28) Lodge, T. P.; Pudil, B.; Hanley, K. J. *Macromolecules* **2002**, *35*, 4707.
- (29) Huang, H. Y.; Remsen, E. E.; Kowalewski, T.; Wooley, K. L. *J. Am. Chem. Soc.* **1999**, *121*, 3805.
- (30) Ma, Q. G.; Remsen, E. E.; Kowalewski, T.; Wooley, K. L. *J. Am. Chem. Soc.* **2001**, *123*, 4627.
- (31) Perkin, K. K.; Turner, J. L.; Wooley, K. L.; Mann, S. *Nano Lett.* **2005**, *5*, 1457.
- (32) Sohn, B. H.; Choi, J. M.; Yoo, S. I.; Yun, S. H.; Zin, W. C.; Jung, J. C.; Kanehara, M.; Hirata, T.; Teranishi, T. *J. Am. Chem. Soc.* **2003**, *125*, 6368.
- (33) Webber, G. B.; Wanless, E. J.; Armes, S. P.; Biggs, S. *Faraday Discuss.* **2005**, *128*, 193.
- (34) Hermans, T. M.; Choi, J.; Lohmeijer, B. G. G.; Dubois, G.; Pratt, R. C.; Kim, H.-C.; Waymouth, R. M.; Hedrick, J. L. *Angew. Chem., Int. Ed.* **2006**, accepted.

NL0612906